Numerical calculations on optical localization in multilayer structures with random-thickness layers

A. Kondilis and P. Tzanetakis
Physics Department, University of Crete, Crete, Greece
and Institute of Electronic Structure and Laser, Foundation for Research and Technology, Hellas, P.O. Box 1527, GR-71110 Heraklion, Greece

(Received 24 February 1992; revised manuscript received 25 June 1992)

A study of localization effects in random, one-dimensional optical systems is presented, based on calculations in superlattices with random-thickness layers. A numerical treatment of the problem of electromagnetic wave propagation in these systems is employed with a transfer-matrix formalism. A localization length l is determined numerically in each case. In order to ensure that the computation results have more general validity in as wide a range of wavelengths as possible, there was no restriction imposed on the number of layers necessary to obtain the value of l with a given accuracy. Appropriate dimensionless variables have been used that greatly simplify the presentation of results. The numerical calculation gives interesting hints about the dependence of the localization length on the gap structure of the corresponding regular superlattice, i.e., the one formed by reducing to zero the standard deviation of layer thickness. This dependence is more intricate than a simple broadening of the regular's gaps, a creation of band tails, induced by disorder.

I. INTRODUCTION

The propagation of light in random media is a topic that has recently received considerable attention.[1-7] The work presented here is the continuation and generalization of calculations we have performed[8] that have successfully accounted for features observed experimentally on the reflection spectra of amorphous multilayer structures, consisting of alternating "well" (w) layers of a-Si:H and "barrier" (b) layers of a-$Si_{1-x}N_x$:H.[9,10] In the previously mentioned studies, the well layers had thicknesses chosen randomly from a Gaussian distribution. In this case, the randomness parameter is the standard deviation σ_{dw} of the well layer thickness distribution.

The study mentioned above[8] and subsequent publications[11] have raised several important questions regarding the effect of electromagnetic wave *localization* in random superlattices. We use the term localization to denote an exponential attenuation of wave amplitude versus depth that is not due to absorption. This effect is often referred to as *strong localization*. In the first place, it is not clear when this term can be used to describe phenomena observed in the reflectance and transmittance spectra of random multilayer structures. In this respect, the number of layers in the superlattice may not be the only relevant parameter that sets a border line, even a vague one, between microscopic and macroscopic systems. In the former, it is more appropriate to speak about random interference effects, whereas, in the latter, localization can be detected unambiguously.

A second group of questions concerns the dependence of the localization length on the frequency of light. Does this dependence follow a predictable pattern? What are the energy regions that are most affected by disorder? Are there particular energies at which, for a given random sequence, the localization length is much lower or much higher than that of neighboring energies?

A third question is related to the interplay of three different effects resulting in exponential attenuation of the wave in the superlattice, namely, Bragg reflection (optical band gaps), disorder, and absorption.

II. ASSUMPTIONS AND METHODS OF CALCULATION

The multilayer structures or superlattices studied consist of alternating layers of lower and higher index material termed "barrier" and "well" layers, respectively. In order to make the numerical calculations more realistic, we have considered a superlattice (SL) deposited on a dielectric substrate. In each case, we have been interested in three SL's related to each other: the *regular* that has well and barrier layers with constant thickness d_w and d_b, the *random well* that has constant thickness d_b for all the barrier layers and well layers with thickness $d_{w,k}$ (k is the layer pair index) chosen randomly from a Gaussian distribution around d_w and, finally, the *all random* that has random thicknesses, around the values of the corresponding regular, for both types of layers.

In the absence of absorption, regular superlattices exhibit frequency spectra with regions of free propagation for the wave interrupted by photonic gaps. Within the gaps, the mean value of amplitude envelope of the wave decays exponentially with depth. This is not an exact statement since the mean envelope in the same layer is constant. Nevertheless, if we plot it versus the distance from the free surface of any given position within the superlattice period, we find an exponential variation.

The mean amplitude envelope decays exponentially with depth at any frequency in all the random superlattices studied. Since we are interested in the effect of ran-

domness on wave propagation both outside and within the gaps of the corresponding regular SL, we use the term localization length to denote the decay constant for both random and regular SL's.

All calculations presented assume normal incidence of light. We start from the "exit" surface: the interface between the SL and the substrate. This interface is the origin of an axis z having direction opposite to that of the incident wave.

We follow the evolution of the electric field inside the medium using *refraction* and *phase matrices*.[12] A phase matrix is defined by

$$\begin{bmatrix} E_m'^{+} \\ E_m'^{-} \end{bmatrix} = U_m \begin{bmatrix} E_m^{+} \\ E_m^{-} \end{bmatrix} , \tag{1}$$

where m denotes a layer of either well or barrier type, the E's are the electric field components at one end of the layer, the one that is closer to the substrate, and the E''s are the components at the other end. The plus/minus signs designate waves traveling in opposite directions. The plus sign labels the wave component traveling in the direction of incidence.

A refraction matrix at the interface between layers $m-1$ and m is defined by

$$\begin{bmatrix} E_m^{+} \\ E_m^{-} \end{bmatrix} = W_{m-1/m} \begin{bmatrix} E_{m-1}'^{+} \\ E_{m-1}'^{-} \end{bmatrix} . \tag{2}$$

In most of the calculations, we have assumed inside the substrate a zero value for the reflected component (superscript minus) of the electric field and unity value for the transmitted. It was verified that neither this assumption nor the substrate index affect in any significant way the results obtained for l.

The refraction matrix has the form

$$W_{m-1/m} = \frac{1}{2} \begin{bmatrix} 1+n_{m-1}/n_m & 1-n_{m-1}/n_m \\ 1-n_{m-1}/n_m & 1+n_{m-1}/n_m \end{bmatrix} \tag{3}$$

and the phase matrix is

$$U_m = \begin{bmatrix} e^{i\varphi_m} & 0 \\ 0 & e^{-i\varphi_m} \end{bmatrix} , \tag{4}$$

where n_m and φ_m are, respectively, the refractive index and phase shift inside layer m.

The electric-field amplitude oscillates with z inside the SL. In order to determine the localization length, we first find the positions and values of the extrema of the electric-field amplitude. Next, we compute the mean envelope amplitude E_0. It is defined as the mean value between one maximum or minimum and the linear interpolation between its adjacent minima or maxima, respectively. This value is attributed to the z position of the central extremum. l is obtained from linear regression on $\log_e(E_0)$ versus z, in a range of 8 orders of magnitude of E_0. This range may, *a priori*, seem excessively large for the determination of an average exponential decay length. It becomes evident in the analysis of the computation results that follows that it is not.

In the case of random SL's, the results may depend on the particular random sequence (RS) used for the calculation. Nevertheless, in plotting and comparing results for different RS's, convenient combinations of the average thicknesses $\langle d_w \rangle$, $\langle d_b \rangle$, the standard deviations δd_w, δd_b of the layers and the refractive indices n_w, n_b can be used. As can be seen from (3) and (4), it is the phase shifts and the ratio of indices that enter the calculation. Based on the above remarks, we have chosen the following set of variables: Z, σ_w, σ_b, c_n, φ, c_φ, where

$$Z = z/(\langle d_w \rangle + \langle d_b \rangle) , \tag{5}$$

$$\sigma_w = \delta d_w/(\langle d_w \rangle + \langle d_b \rangle) \tag{6a}$$

and

$$\sigma_b = \delta d_b/(\langle d_w \rangle + \langle d_b \rangle) , \tag{6b}$$

i.e., Z, σ_w, and σ_b are measured in units of the average SL period

$$c_n = n_w/n_b , \tag{7}$$

$$\langle \varphi_b \rangle = \frac{2\pi n_b \langle d_b \rangle}{\lambda} , \tag{8a}$$

and

$$\langle \varphi_w \rangle = \frac{2\pi n_w \langle d_w \rangle}{\lambda} , \tag{8b}$$

where λ is the vacuum wavelength of light.

$$c_\varphi = \langle \varphi_w \rangle / \langle \varphi_b \rangle . \tag{9}$$

Finally, in order to simplify the notation we take

$$\varphi = \langle \varphi_b \rangle . \tag{10}$$

The localization length l is also expressed in units of the average SL period. A value of 2 for c_n is used in all calculations presented here.

III. COMPUTATION RESULTS FOR THE LOCALIZATION LENGTH

Figure 1 shows a typical semilogarithmic plot of $E_0(z)$ in a case of relatively weak localization. Despite the large fluctuations observed, the overall exponential variation with depth is apparent. A linear fit on these data yields a localization length of 3250 average SL periods. There are regions in the random-thickness sequence where the wave propagates more freely than in others. The size of these regions can be large compared to l. In the lower left part of Fig. 1, one such region extends over about 15 000 SL periods. The extent of and average wave attenuation in these regions depend on the particular random sequence used.

We have found that the best way to identify, unambiguously, an exponential decay and to determine with confidence l is not to restrict the number of layers that enter the calculation, but to stop when the ratio of entrance to exit amplitudes has reached a given value. We have chosen 10^8 as a sensible compromise between accuracy and computation length. In the case of large σ_w, near the gap edges, l is of the order of 10. The number of

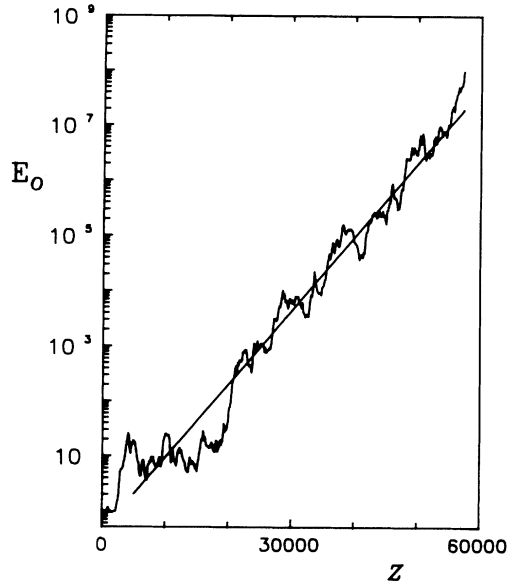

FIG. 1. Mean amplitude envelope E_0 vs distance from the substrate-superlattice interface, for a random-well superlattice. $c_n=2$, $c_\varphi=1$, $\varphi=0.05\pi$, $\sigma_w=10/60$ (see text for symbols). The localization length, calculated by linear regression on this curve, is 3250 average SL periods. Z is expressed in average SL periods.

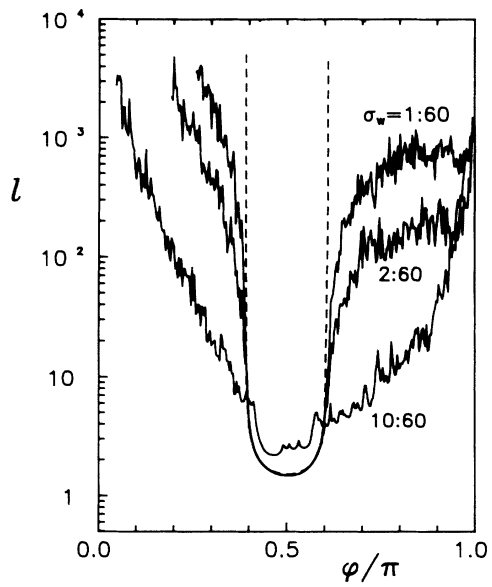

FIG. 2. Localization length l in units of the average SL period, vs φ in the first zone ($0<\varphi<\pi$), for three random-well SL's with different normalized thickness standard deviation σ_w shown with each curve. $c_\varphi=1$ and $c_n=2$. The dashed curve is the plot of $l(\varphi)$ for the corresponding regular SL.

layers that correspond to a ratio of 10^8 decreases significantly and l obtained may be strongly dependent on the particular sequence. We have verified, then, that ratios of 10^{16} and 10^8 yield similar values for l.

It is expected that $l(h\nu)$ or $l(\varphi)$ in the units we have defined above depends strongly on the proximity of a photonic gap. In a regular SL with two types of layers, one can distinguish between *tuned* and *detuned* structures.[12] Tuned SL's have a ratio c_φ that is the quotient of two small integers. We have studied the effect of disorder in random well SL's with corresponding regulars that belong to two representative cases: (i) the simplest tuned with $c_\varphi=1$ and (ii) a detuned SL with $c_\varphi=0.63$. In the following, we refer to the φ ranges: 0 to π and π to 2π as the first and second zone, respectively. The tuned SL with $c_\varphi=1$ has the simplest gap structure with one gap centered in each zone. This holds for higher-order zones also. On the contrary, the detuned SL does not have the same gap structure in each zone. A periodicity in this φ space may appear for much larger φ's if the ratio c_φ is a rational number. For disordered SL's, the dependence of $l(\varphi)$ from the proximity of gaps can be illustrated very well in the first two zones. We restrict the presentation of results within this range.

Figure 2 shows the computed l in the first zone for three random-well SL's with standard deviations: $\sigma_w=1/60$, $\sigma_w=2/60$, and $\sigma_w=10/60$. The average SL period is tuned with $c_\varphi=1$. The dashed curve is the plot of l values calculated for the corresponding regular SL. The photonic gap has very sharp edges. Outside the gap l is infinite. For the random SL's, l follows a regular pattern despite fluctuations. The strongest localization appears in the gap and its immediate vicinity with the formation of tails on the gap edges. Inside the gap, disorder induces a small increase of l. Between gaps, very small disorder induces relatively strong localization. l appears to reach a plateau (for $\sigma_w=1/60$ and $\sigma_w=2/60$), interrupted by a singularity at $\varphi=\pi$. The existence of this plateau is discussed below, along with the presentation of the results obtained for the detuned SL's.

At the boundary between zones, where φ is an integer multiple of π, l goes to infinity. This is a photon energy at which light propagates freely in a random-well superlattice of any number of layers. The explanation of this singularity is very simple: When the barrier layer thickness is constant and the phase shift inside it is equal to an integer multiple of π, the barrier layer phase matrices become unit matrices times ±1. Consequently, in the layer matrix product, that is, the system transfer matrix, two consecutive well layer phase matrices are separated by a unit phase matrix and two refraction matrices which are inverse to each other. The result is that their product is equivalent to the phase matrix of one well layer having thickness equal to the sum of the two-well-layer thicknesses. One can then consider the medium as consisting entirely of well material. A ±1 factor for the whole is of no importance to the determination of the electric-field amplitude. For convenience, in the following, we refer to the singularity at $\varphi=k\pi$, where k is an integer, as an *antigap*. An interesting observation is that the width of the antigap broadens significantly with increasing disorder.

As mentioned above, it is expected that l does depend on the particular sequence used in the calculation. This is especially true if the number of layers entering a calculation is necessarily limited, as is the case when l has a value of the order of 10. We have plotted in Fig. 3 l

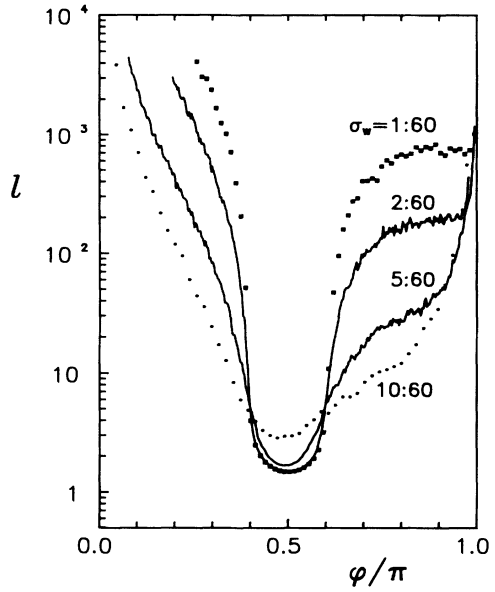

FIG. 3. Average localization length l in the first zone. Each data point is obtained by averaging over 20 different random-well SL's all having the same σ_w. Other parameters are identical to those of Fig. 2. The normalized standard deviation σ_w of the well layer thickness is shown with each curve.

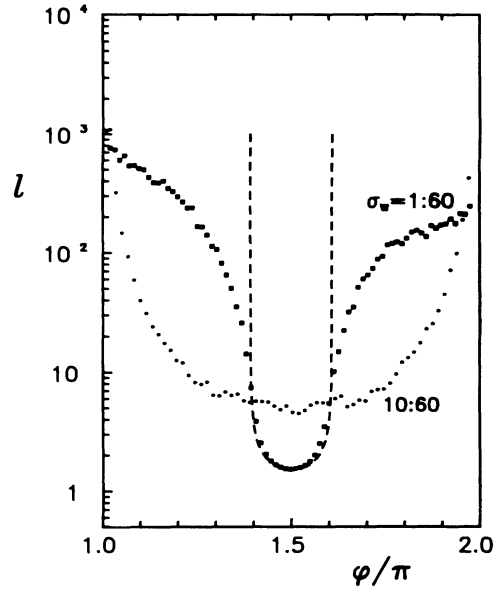

FIG. 4. Average localization length l, over 20 different sequences, in the second zone for two values of σ_w. All other parameters are identical to those of Figs. 2 and 3. The dashed line shows $l(\varphi)$ for the corresponding regular SL.

values that are the average of those computed for 20 different random sequences with all other conditions identical. In comparing the curves of Fig. 3 to those of Fig. 2, one observes much lower fluctuations in the average l plots. On the other hand, all the general features of $l(\varphi)$ are the same for a single random sequence and for the average curves.

IV. DISORDER AND PHASE SHIFTS OF THE WAVE INSIDE THE LAYERS

The behavior of l in the second zone, as can be seen in Fig. 4, is qualitatively similar to that in the first one. The effect of a given randomness is stronger. This is expected if one considers that the important parameter is not σ_w but $\sigma_{\varphi w}$, the standard deviation of phase shifts φ_w. One expects an increasing effect as a wider range of *well layer phases* enters the calculation, either by increasing σ_w or by increasing φ_w. Indeed, the curve for $\sigma_w=2/60$ of Fig. 3 in the upper half of the first zone is almost identical to that for $\sigma_w=1/60$ in Fig. 4 in the upper half of the second zone. In this respect, for a given σ_w, there should be a saturation in the localization effect at photon energies large enough to give $\sigma_{\varphi w}$ of the order of π.

There is a more general relationship between l computed in different zones with different standard-thickness deviations. The following derivation is valid even when both layers have thickness varying randomly. It assumes that c_n is constant. Let us separate the phase shift, e.g., inside a barrier layer m, into two parts:

$$\varphi_m=\langle\varphi_m\rangle+\Delta\varphi_m \ , \tag{11a}$$

with mth barrier layer thickness

$$d_m=\langle d_m\rangle+\Delta d_m \ . \tag{11b}$$

We observe that phase matrices remain invariant or are multiplied by -1 (which has no effect on l) if we change the average barrier phase by an integer multiple of π, without affecting the $\Delta\varphi_m$'s. It can be easily verified that the localization length computed for a given SL for $\langle\varphi_m\rangle$ is identical to that computed for $\langle\varphi'_m\rangle=\langle\varphi_m\rangle+k\pi$ in another SL whose barrier layers have thickness deviations $\Delta d'_m$ given by

$$\Delta d'_m=\begin{bmatrix} \langle\varphi_m\rangle/\pi & \langle d'_m\rangle \\ \langle\varphi_m\rangle/\pi+k & \langle d_m\rangle \end{bmatrix}\Delta d_m \ ,$$

hence,

$$\delta d'=\begin{bmatrix} \langle\varphi_m\rangle/\pi & \langle d'_m\rangle \\ \langle\varphi_m\rangle/\pi+k & \langle d_m\rangle \end{bmatrix}\delta d \ , \tag{13}$$

where δd's are the standard deviations of Δd_m's. Identical relations hold for the well layers.

Since, as we have pointed out above, the general behavior of l does not depend on the particular sequence, we expect it to depend only on the distribution parameters. In conclusion, using the set of dimensionless variables define by relations (5)–(10), we expect l to be invariant under the transformations

$$\varphi'=\varphi+k\pi \ , \tag{14}$$

$$\sigma'_b=A\sigma_b \ , \tag{15a}$$

$$\sigma'_w=A\sigma_w \ , \tag{15b}$$

where

$$A=\frac{\varphi/\pi(c_n+c_\varphi)}{(\varphi/\pi+k)(c_n+c'_\varphi)} \tag{16}$$

and

$$c'_\varphi=\frac{\varphi/\pi}{\varphi/\pi+k}c_\varphi+\frac{\mu}{\varphi/\pi+k}\ , \tag{17}$$

k,μ are integers.

As we have pointed out above, the curve for $\sigma_w=2/60$ (Fig. 3) at the end of the first zone and the curve for $\sigma_w=1/60$ (Fig. 4) at the end of the second zone are similar. This is one example of l invariance under the above transformations with $c_\varphi=c'_\varphi=1$ and $\mu=k=1$.

In the case of all random SL's with tuned regular, we have obtained results that are similar to those presented in Figs. 3 and 4 with the exception of the antigap singularities at $\varphi=\pi,2\pi$. When σ_b is low, one can still observe small peaks that are the remnants of the antigaps of the *random-well* case. These peaks disappear with increasing σ_b. If disorder is strong, the variation of l with energy shows two distinct regimes: the low-frequency end, characterized by a rapid decrease of l with increasing $h\nu$, followed, at higher frequencies by a region where $l(\varphi)$ depends on the underlying gap structure of the corresponding regular SL but remains close to 10 SL periods. This value is very close to those found for large disorder, for two different random SL models, by Sheng.[7]

Figure 5 shows the results obtained for detuned SL's. One can observe a qualitative difference in the behavior of l when comparing the curve for the random SL in Fig. 5 to those with $\sigma_w=1/60$ in Figs. 3 and 4. The disorder parameter is almost identical, but the clear plateau and the very narrow antigap of the tuned case are absent. l values in the vicinity of $\varphi=\pi$ are much higher for $c_\varphi=0.63$ (Fig. 5) than for $c_\varphi=1$ (Figs. 3 and 4). At first sight, one is surprised by the difference in the behavior of

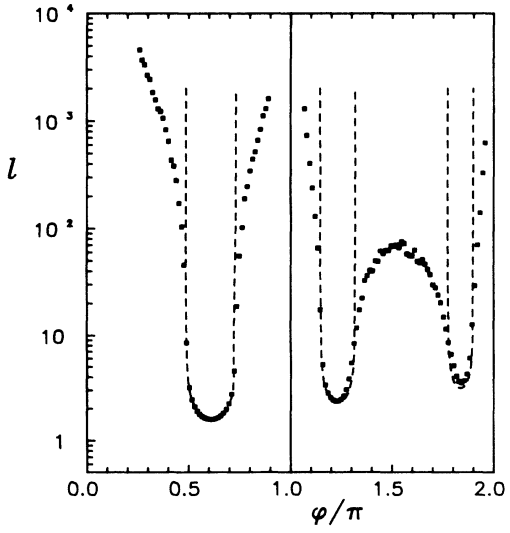

FIG. 5. Average l, over 20 sequences, vs average barrier layer phase shift φ in the first two zones, for random-well SL's with detuned equivalent regular. $\sigma_w=0.019$, $c_\varphi=0.63$, $c_n=2$. The dashed line is the plot of $l(\varphi)$ for the regular SL.

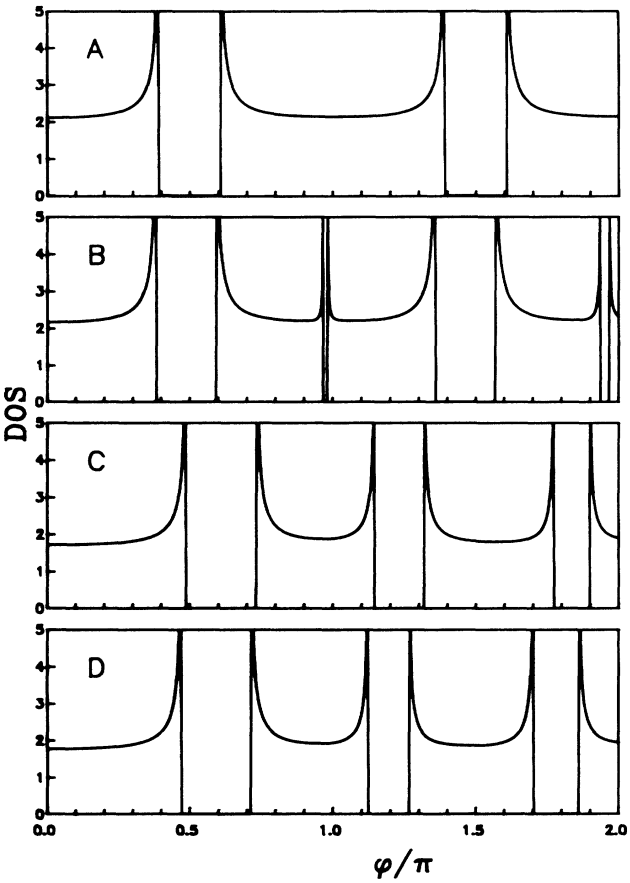

FIG. 6. Density of states, per SL period, of tuned and detuned regular superlattices vs phase shift φ of the wave inside the barrier layer. In all graphs $c_n=2$. *A*, $c_\varphi=1$; *B*, $c_\varphi=1.05$; *C*, $c_\varphi=0.63$; and *D*, $c_\varphi=0.68$.

l between two consecutive gaps in these two cases. There is, nevertheless, a fundamental difference in the gap structure of the two corresponding regular SL's in the first two zones. This difference is illustrated in Fig. 6, with graphs of the density of states[13] versus φ for regular SL's with $c_\varphi=1$, graph *A*, and $c_\varphi=1.05$, graph *B*.

We observe that the small deviation from $c_\varphi=1$ creates a third narrow photonic gap just below $\varphi=\pi$ (and $\varphi=2\pi$). A similar gap above $\varphi=\pi$ appears for c_φ slightly lower than 1. Disorder creates a random detuning around $c_\varphi=1$ that is responsible for the plateau close to $\varphi=\pi$ in Fig. 3. On the contrary, small deviations from $c_\varphi=0.63$ do not result in the creation of any gap around $\varphi=\pi$, as one can see by comparing graphs *C* and *D* of Fig. 6. The energy dependence of l close to $\varphi=\pi$ for $c_\varphi=0.63$ (Fig. 5), reflects only the creation of tails on the edges of the gaps.

V. THE ROLE OF ABSORPTION

The formalism and computational method we have used are not restricted to real refractive indices. The combined effect of disorder and absorption can be readily investigated without simplifying assumptions. We have

performed a series of calculations with a nonzero imaginary part for n_w covering many phases of φ outside the gaps of the corresponding regular. The imaginary part of n_w, in each case, was chosen in such a way that the decay length inside the corresponding regular in the presence of absorption (the inelastic l without disorder: $l_{0,i}$), was not very different from l, the decay length of the random SL in the absence of absorption. The inelastic decay constant l_i in the random SL, as well as $l_{0,i}$, was computed in exactly the same manner as previously described for l. In order to test the interdependence of disorder and absorption, we have computed in each case a localization length l_c using the formula

$$\frac{1}{l_c}=\frac{1}{l_i}-\frac{1}{l_{0,i}} , \tag{18}$$

which, applied to l's that are of the same order of magnitude, should yield a value close to the localization length, if disorder and absorption are independent.

We have considered the random well case with $\sigma_w=1/60$ and $\sigma_w=10/60$. The values of decay constants were obtained by averaging over 20 SL's differing only in the random-thickness sequence used. Several values of φ in the first zone were tested. The relative difference $|l-l_c|/l$ we have found in all cases was less than 15% and, more often, lower than 5%.

VI. CONCLUSIONS

A series of numerical calculations of the localization length l in various, random-thickness, multilayer structures with two types of layers has been performed. The picture emerging from these calculations, when disorder is weak, is that the variation of the localization length with photon energy closely relates to the gap structure of the corresponding regular superlattices. A finite localization length is found at all nonzero photon energies, with the exception of multilayers having rigorously constant thickness for one type of layer and random for the other. There are frequencies, then, at which the wave propagates freely no matter how strong the thickness fluctuations are. The trends in the frequency dependence of l we have found for large disorder are in good qualitative agreement with previous studies of randomly layered systems with different types of disorder. Finally, it was shown that absorption and disorder have independent effects on wave attenuation in the structures studied.

ACKNOWLEDGMENT

The authors are grateful to Professor E. N. Economou for valuable discussions throughout the progress of the work presented here.

[1]E. Sendler and D. G. Steel, J. Opt. Am. B **5**, 1636 (1988).
[2]M. P. van Albada, M. B. van der Mark, and A. Lagendijk, Phys. Rev. Lett. **58**, 361 (1987).
[3]M. M. Sigalas and E. N. Economou (unpublished).
[4]E. N. Economou and C. M. Soukoulis, Phys. Rev. B **40**, 7977 (1989).
[5]K. M. Ho, C. T. Chan, and C. M. Soukoulis, Phys. Rev. Lett. **65**, 3152 (1990).
[6]J. Igarashi, J. Phys. Soc. Jpn. **57**, 3391 (1988).
[7]*Scattering and Localization of Classical Waves in Random Media,* edited by P. Sheng (World Scientific, Singapore, 1990).
[8]A. Kondilis and P. Tzanetakis, Philos. Mag. Lett. **62**, 299 (1990).
[9]S. Nitta, T. Itoh, S. Nonomura, H. Ohta, and K. Morigaki, Philos. Mag. B **60**, 119 (1989).
[10]T. Itoh, S. Nitta, and S. Nonomura, J. Non-Cryst. Solids **114**, 723 (1989).
[11]S. Nitta, S. Takeuchi, K. Ogawa, T. Furukawa, T. Itoh, and S. Nonomura, J. Non-Cryst. Solids **137&138**, 1095 (1991).
[12]Z. Knittl, *Optics of Thin Films* (Wiley, New York, 1976).
[13]The density of states is calculated using Bloch's theorem, in a way analogous to that of the one-dimensional electronic case of the Kronig-Penney model.